Two-mode multiplexing at 2 × 10.7 Gbps over a 7-cell hollow-core photonic bandgap fiber

Xu, Jing; Peucheret, Christophe; Lyngsø, Jens Kristian ; Leick, Lasse

Published in:
Optics Express

Link to article, DOI:
10.1364/OE.20.012449

Publication date:
2012

Document Version
Publisher's PDF, also known as Version of record

Citation (APA):
Xu, J., Peucheret, C., Lyngsø, J. K., & Leick, L. (2012). Two-mode multiplexing at 2 × 10.7 Gbps over a 7-cell hollow-core photonic bandgap fiber. Optics Express, 20(11), 12449-12456. DOI: 10.1364/OE.20.012449

Two-mode multiplexing at 2 × 10.7 Gbps over a 7-cell hollow-core photonic bandgap fiber

Jing Xu,[1,*] Christophe Peucheret,[1] Jens Kristian Lyngsø,[2] and Lasse Leick[2]

[1]*DTU Fotonik, Department of Photonics Engineering, Technical University of Denmark, DK-2800 Kgs. Lyngby, Denmark*

[2]*NKT Photonics A/S, Blokken 84, DK-3460 Birkerød, Denmark*

[*]*jinxu@fotonik.dtu.dk*

Abstract: Current technologies are fast approaching the capacity limit of single mode fibers (SMFs). Hollow-core photonic bandgap fibers (HC-PBGFs) are expected to provide attractive long-term solutions in terms of ultra-low fiber nonlinearities associated with the possibility of mode scaling, thus enabling mode division multiplexing (MDM). In this work, we demonstrate MDM over a HC-PBGF for the first time. Two 10.7 Gbps channels are simultaneously transmitted over two modes of a 30-m long 7-cell HC-PBGF. Bit error ratio (BER) performances below the FEC threshold limit (3.3×10^{-3}) are shown for both data channels when the two modes are transmitted simultaneously. No power penalty and up to 3 dB power penalty at a BER of 10^{-9} are measured for single mode transmission using the fundamental and the LP_{11} mode, respectively. The performance of this exploratory demonstration is expected to improve significantly if advanced mode launching and detection methods are used.

OCIS codes: (060.2270) Fiber characterization; (060.2330) Fiber optics communications.

References and links

1. S. Schöllmann, N. Schrammar, and W. Rosenkranz, "Experimental realisation of 3×3 MIMO system with mode group diversity multiplexing limited by modal noise," in the *Optical Fiber Communication Conference and Exposition (OFC) and the National Fiber Optic Engineers Conference (NFOEC)*, OSA Technical Digest (CD) (Optical Society of America, 2008), paper JWA68.
2. C. P. Tsekrekos, M. de Boer, A. Martinez, F. M. J. Willems, and A. M. J. Koonen, "Demonstration of a Transparent 2-Input 2-Output Mode Group Diversity Multiplexing Link," in the *European Conference on Optical Communications* (Cannes, France, 2006), paper We3.P.145.
3. N. Hanzawa, K. Saitoh, T. Sakamoto, T. Matsui, S. Tomita, and M. Koshiba, "Demonstration of mode-division multiplexing transmission over 10 km two-mode fiber with mode coupler," in the *Optical Fiber Communication Conference and Exposition (OFC) and the National Fiber Optic Engineers Conference (NFOEC)*, OSA Technical Digest (CD) (Optical Society of America, 2011), paper OWA4.
4. A. Al Amin, A. Li, S. Chen, X. Chen, G. Gao, and W. Shieh, "Dual-LP_{11} mode 4×4 MIMO-OFDM transmission over a two-mode fiber," Opt. Express **19**(17), 16672–16679 (2011).
5. C. Koebele, M. Salsi, D. Sperti, P. Tran, P. Brindel, H. Mardoyan, S. Bigo, A. Boutin, F. Verluise, P. Sillard, M. Astruc, L. Provost, F. Cerou, and G. Charlet, "Two mode transmission at 2×100 Gb/s, over 40 km-long prototype few-mode fiber, using LCOS-based programmable mode multiplexer and demultiplexer," Opt. Express **19**(17), 16593–16600 (2011).
6. R. Ryf, S. Randel, A. H. Gnauck, C. Bolle, A. Sierra, S. Mumtaz, M. Esmaeelpour, E. C. Burrows, R.-J. Essiambre, P. J. Winzer, D. W. Peckham, A. H. McCurdy, and R. Lingle, "Mode-division multiplexing over 96 km of few-mode fiber using coherent 6×6 MIMO processing," J. Lightwave Technol. **30**(4), 521–531 (2012).
7. N. Bai, E. Ip, Y.-K. Huang, E. Mateo, F. Yaman, M.-J. Li, S. Bickham, S. Ten, J. Liñares, C. Montero, V. Moreno, X. Prieto, V. Tse, K. Man Chung, A. P. T. Lau, H.-Y. Tam, C. Lu, Y. Luo, G.-D. Peng, G. Li, and T. Wang, "Mode-division multiplexed transmission with inline few-mode fiber amplifier," Opt. Express **20**(3), 2668–2680 (2012).
8. M. N. Petrovich, F. Poletti, A. van Brakel, and D. J. Richardson, "Robustly single mode hollow core photonic bandgap fiber," Opt. Express **16**(6), 4337–4346 (2008).
9. J. K. Lyngsø, B. J. Mangan, C. Jakobsen, and P. J. Roberts, "7-cell core hollow-core photonic crystal fibers with low loss in the spectral region around 2 µm," Opt. Express **17**(26), 23468–23473 (2009).
10. http://nktphotonics.com/files/files/HC-1550-04-100409.pdf
11. B. Mangan, L. Farr, A. Langford, P. J. Roberts, D. P. Williams, F. Couny, M. Lawman, M. Mason, S. Coupland, R. Flea, H. Sabert, T. A. Birks, J. C. Knight, and R. S. J. Philip, "Low loss (1.7 dB/km) hollow core photonic

bandgap fiber," in *Optical Fiber Communication Conference*, Technical Digest (CD) (Optical Society of America, 2004), paper PD24.
12. P. J. Roberts, F. Couny, H. Sabert, B. J. Mangan, D. P. Williams, L. Farr, M. W. Mason, A. Tomlinson, T. A. Birks, J. C. Knight, and P. St. J. Russell, "Ultimate low loss of hollow-core photonic crystal fibres," Opt. Express **13**(1), 236–244 (2005).
13. C. Peucheret, B. Zsigri, T. P. Hansen, and P. Jeppesen, "10 Gbit/s transmission over air-guiding photonic bandgap fibre at 1550 nm," Electron. Lett. **41**(1), 27–29 (2005).
14. P. J. Roberts, D. P. Williams, H. Sabert, B. J. Mangan, D. M. Bird, T. A. Birks, J. C. Knight, and P. St. J. Russell, "Design of low-loss and highly birefringent hollow-core photonic crystal fiber," Opt. Express **14**(16), 7329–7341 (2006).
15. B. Mangan, J. K. Lyngsø, and P. J. Roberts, "Realization of low loss and polarization maintaining hollow core photonic crystal fibers," in *Conference on Lasers and Electro-Optics/Quantum Electronics and Laser Science Conference and Photonic Applications Systems Technologies*, OSA Technical Digest (CD) (Optical Society of America, 2008), paper JFG4.
16. http://www.jcmwave.com
17. T. G. Euser, G. Whyte, M. Scharrer, J. S. Y. Chen, A. Abdolvand, J. Nold, C. F. Kaminski, and P. St. J. Russell, "Dynamic control of higher-order modes in hollow-core photonic crystal fibers," Opt. Express **16**(22), 17972–17981 (2008).
18. J. West, C. Smith, N. Borrelli, D. Allan, and K. Koch, "Surface modes in air-core photonic band-gap fibers," Opt. Express **12**(8), 1485–1496 (2004).
19. K. Saitoh, N. Mortensen, and M. Koshiba, "Air-core photonic band-gap fibers: the impact of surface modes," Opt. Express **12**(3), 394–400 (2004).
20. P. Pepeljugoski, S. E. Golowich, A. J. Ritger, P. Kolesar, and A. Risteski, "Modeling and simulation of next-generation multimode fiber links," J. Lightwave Technol. **21**(5), 1242–1255 (2003).
21. V. R. Daria, P. John Rodrigo, and J. Glückstad, "Programmable complex field coupling to high-order guided modes of micro-structured fibres," Opt. Commun. **232**(1-6), 229–237 (2004).
22. N. V. Wheeler, M. N. Petrovich, R. Slavik, N. K. Baddela, E. R. Numkam Fokoua, J. R. Hayes, D. Gray, F. Poletti, and D. Richardson, "Wide-bandwidth, low-loss, 19-cell hollow core photonic band gap fiber and its potential for low latency data transmission," *in Optical Fiber Communication Conference,* OSA Technical Digest (Optical Society of America, 2012), paper PDP5A.2.

1. Introduction

It has been generally realized that current optical transmission technologies are fast approaching the capacity limit of single mode fibers (SMFs). Mode division multiplexing (MDM) has been recognized as a promising candidate for extending this limit by utilizing the spatial dimension of optical fibers. MDM has been so far demonstrated using graded-index multi-mode fibers (GI-MMFs) [1,2] and few-mode solid-core step-index fibers [3–7], targeting short-range and long-haul applications, respectively. However, one of the practical limitations to the information capacity of systems making use of solid core fibers is fiber nonlinearities. Hollow-core photonic bandgap fibers (HC-PBGFs) may greatly relieve the impact of nonlinearities by supporting light transmission in air for up to 90% or more of the signal power [8–10]. The minimum loss of such fibers depends on the air-filling fraction [11,12]. Lower loss can be achieved by increasing the dimension of the air core, resulting in multi-mode operation [8], which can in turn be exploited for MDM. In addition, HC-PBGFs can be used for opening new transmission windows around 2 μm where their minimum loss, significantly lower than that of solid-core silica fibers in the same wavelength range, has been theoretically predicted [9,11,12]. Even though single-mode transmission over HC-PBGFs has been described in [13], their use in an MDM system has never been reported to date.

In this work, we demonstrate an exploratory two-mode multiplexing system over a 7-cell HC-PBGF. LP_{11} modes are excited by offset-launching light at the input of the HC-PBGF. Different LP_{11} modes can be selectively excited by changing the polarization of the input light. Mode de-multiplexing is realized by carefully selecting the detection position at the fiber output depending on the mode profile. Two 10.7 Gbps non-return to zero (NRZ) signals are transmitted over different LP_{11} modes, namely LP_{11a} and LP_{11b}. Up to 3 dB power penalty at a bit error ratio (BER) of 10^{-9} is measured when transmitting only a single LP_{11} mode. The BER performance when transmitting two LP_{11} modes simultaneously is below the FEC threshold (3.3×10^{-3}) for concatenated codes assuming 7%-overhead coding. The large sensitivity degradation is attributed to the mode de-multiplexing technique, which could be greatly improved by optimizing the detection method.

#166096 - $15.00 USD Received 5 Apr 2012; revised 12 May 2012; accepted 12 May 2012; published 16 May 2012

2. Properties of 7-cell HC-PBGFs

The fiber used in this work is a 7-cell hollow core photonic bandgap fiber with a cladding air filling fraction of roughly 92% [10]. Six antiresonant features are positioned around the core wall, where they promote a reduction in transmission loss by lowering the overlap between the light field and silica surfaces inside the fiber [14,15]. The guided modes and appertaining dispersion profiles were calculated using the commercial finite element solver JCMwave [16]. Only the LP_{11} manifold is considered, which consists of the even and odd HE_{21}, TE_{01} and TM_{01}-like modes.

The electric field distributions of the four higher order core-guided modes in the LP_{11} manifold are sketched in Fig. 1(a). Due to the symmetry of these modes and the launch mechanism used in this work, they are commonly excited in pairs. Consequently, the observed output fields, named LP_{11a} and LP_{11b}, are each a superposition of two modes as depicted in Fig. 1(b).

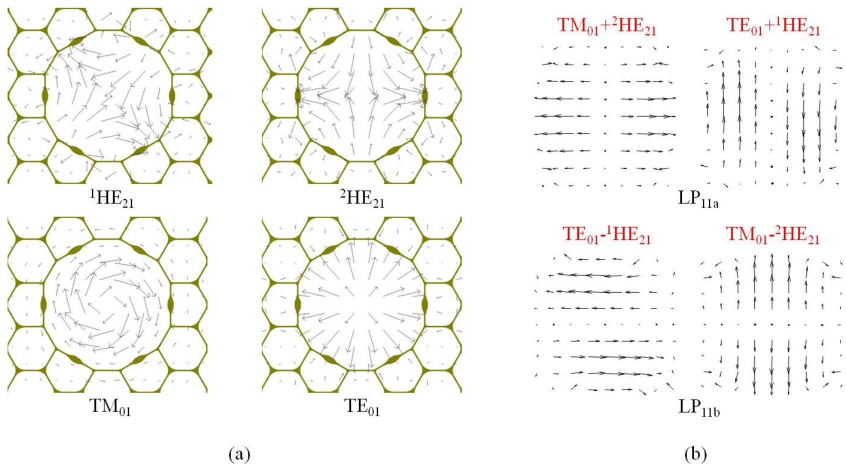

Fig. 1. (a) In plane vector field representation of the four modes in the LP_{11} manifold. (b) Superpositions of modes contributing to the LP_{11a} and LP_{11b} modes.

The nominal loss of the fundamental mode is ~11 dB/km. The transmission loss of the modes in the LP_{11} manifold depends on the specific fiber design and can be challenging to quantify due to the presence of the low loss fundamental mode [17]. Our calculations suggest that especially the TE_{01} mode is well guided, which is also evident from the mode plots in Fig. 1(a). But since the four modes have a similar spatial profile and comparable effective indices, some intermodal coupling is expected. In the current fiber we have estimated the average transmission loss of the LP_{11} modes to be approximately 4-5 times higher than that of the fundamental mode and thus roughly 50 dB/km.

#166096 - $15.00 USD Received 5 Apr 2012; revised 12 May 2012; accepted 12 May 2012; published 16 May 2012

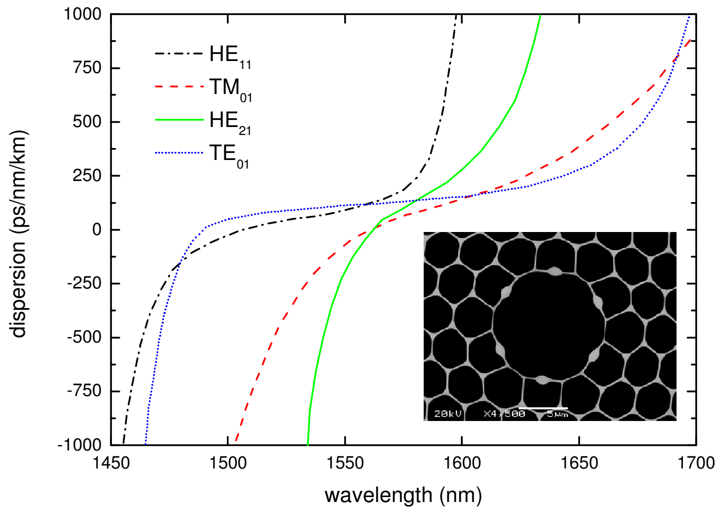

Fig. 2. Calculated dispersion profiles of the modes in the LP_{11} manifold. The inset shows a scanning electron microscope (SEM) picture of the cross section of the 7-cell HC-PBGF.

The group velocity dispersion (GVD) of hollow core fiber modes is dominated by waveguide dispersion and can be strongly affected by mode crossings between modes of similar symmetry, e.g. a core mode and a mode receding in the core wall (surface mode) [18,19]. The exact spectral position of surface modes depends on how the fiber fuses during fabrication and can be difficult to predict by numerical calculations. GVD for the fundamental mode in a 7-cell hollow core fiber typically evolves from normal to anomalous with a D parameter of roughly 100 ps/nm/km at the bandgap center [10]. The zero dispersion wavelength of the fundamental mode of the current fiber is $\lambda_0 = 1500$ nm.

Overall, the dispersion profiles of the LP_{11} modes are similar to the dispersion profile of the fundamental mode but shifted towards longer wavelengths. As shown in Fig. 2 our calculations suggest that the zero dispersion wavelength of the majority of LP_{11} modes is located close to 1550 nm.

3. Two-mode multiplexing and demultiplexing

Figure 3(a) shows the principle of the two-mode multiplexing and demultiplexing method used in this work. The input signal is launched into the HC-PBGF via a piece of tapered SMF. The minimum spot size at the output of the tapered SMF is 2.5 µm. The core diameter of the 7-cell HC-PBGF is 10.6 ± 0.3 µm [10]. The mode profile at the output of the HC-PBGF is first imaged by a 40 times microscope objective and then focused by a 10 times microscope objective into a flat-cut standard SMF (SSMF). Therefore, the mode profile seen by the flat-cut SSMF is roughly 4 times larger than that at the output of the HC-PBGF. In the light path between the two microscope objectives, 50% of the light is reflected by a beam splitter into an infrared camera. The fundamental mode, LP_{01}, can be excited by aligning the tip of the tapered SMF to the center of the HC-PBGF core, as shown in Fig. 3(b) representing the mode profile captured by the camera. LP_{11} modes can be excited by offsetting the first tapered SMF 6 µm away from the center of the HC-PBGF core. By changing the polarization of the input light to the HC-PBGF, two different high order modes, namely the LP_{11a} or the LP_{11b} mode, can be excited, as shown in Figs. 3(c) and 3(d). Figures 3(b)-3(d) were taken with the infrared camera operating in deep-saturation, making the residual power (estimated to less than 1% of the total mode power) residing at the interface between the core and the cladding noticeable as small light spots. The total loss of the HC-PBGF link, including transmission loss and coupling losses from the multiplexing and demultiplexing setup, is measured to be 25 dB for the LP_{01} mode and 40 dB for the LP_{11} modes. Considering the transmission loss discussed in

#166096 - $15.00 USD Received 5 Apr 2012; revised 12 May 2012; accepted 12 May 2012; published 16 May 2012

section 2, the coupling loss of the alignment setup is estimated to be around 24.7 dB and 38.5 dB for the LP_{01} and LP_{11} mode, respectively.

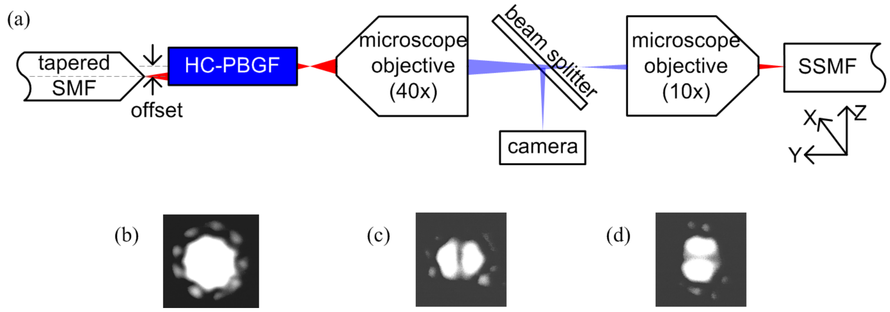

Fig. 3. (a) Schematic view of the two-mode multiplexing and demultiplexing method. (b)-(d) Mode profiles captured by the camera and corresponding to the LP_{01}, LP_{11a}, and LP_{11b} modes, respectively.

The coupling efficiency between the tapered SMF and HC-PBGF is numerically calculated [20] based on the mode profile shown in Fig. 1(b), which is obtained by using a commercial mode solver [16]. The output beam of the tapered SMF is modeled as a Gaussian beam with 1.25 µm beam waist. The beam waist of the tapered SMF is assumed to coincide with the input plane of the HC-PBGF. Figure 4(a) shows the coupling efficiency for the LP_{01} mode (dashed line) and the four LP_{11} modes (solid lines) as a function of the radial offset of the launch position with respect to the centre of the core, normalized to the core radius of the HC-PBGF. The maximum coupling efficiency for the LP_{01} and LP_{11} modes is 0.3 and 0.23 (corresponding to −5.2 dB and −6.4 dB, respectively), peaking at the core center position and half of the core radius, respectively. The extinction ratios, defined as the ratios of the coupling efficiency to the LP_{11} and LP_{01} modes, are shown in Fig. 4(b). The maximum extinction ratios for exciting the LP_{11} modes are obtained when the launch radial offset is close to the value of the fiber core radius, which corresponds to ~5.5 µm. At this position, the coupling efficiencies to the LP_{11} modes are about 0.001 (−30 dB), which is ~25 dB lower than that to the LP_{01} mode at the center launch position. Our coupling calculations explain reasonably well the existence of an optimum launch radial offset found experimentally around 6 µm, as well as the significant difference between the coupling losses to the LP_{01} and LP_{11} modes.

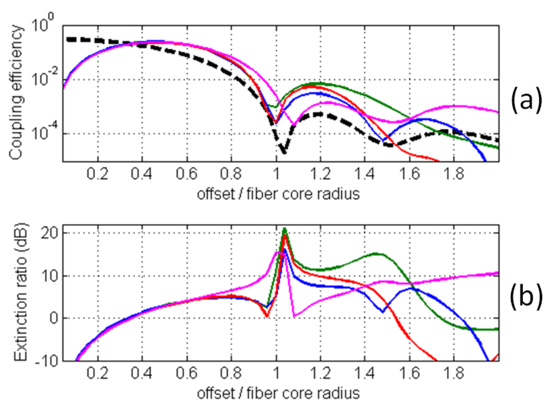

Fig. 4. (a) Calculated coupling efficiency between tapered SMF and HC-PBGF for the LP_{01} (dashed) and LP_{11} modes (solid lines) as a function of normalized radial offset with respect to the core centre. (b) Extinction ratio, defined as the ratio of the coupling efficiencies to the LP_{11} and LP_{01} modes, as a function of radial offset. The radial offset is normalized to the core radius of the HC-PBGF.

#166096 - $15.00 USD Received 5 Apr 2012; revised 12 May 2012; accepted 12 May 2012; published 16 May 2012

Mode de-multiplexing is realized by carefully selecting the detection point on the received mode profiles using a flat-cut SSMF. In our calculations, the output beam of the SSMF is modeled as a Gaussian beam with 5 µm beam waist. The beam waist of the SSMF is assumed to coincide with the image plane of the second microscope objective. The reason why an SSMF is used for light collection instead of a tapered SMF can be seen in Fig. 5(a), which is a contour plot of the calculated coupling efficiency between the mode profile of the HC-PBGF imaged by the second microscope objective and a Gaussian beam profile as a function of radial offset and Gaussian beam waist. The maximum coupling efficiency when using an SSMF is about 0.25, which is about 5 times larger than if a tapered SMF was used. The optimum radial offset in this case is ~12 µm. Figures 5(b) and 5(c) show the calculated and experimental contour plots of the extinction ratio (with respect to the LP_{11b}) for detecting the LP_{11a} mode, respectively. The X and Z directions correspond to the set of axes represented in Fig. 3(a). For the experimental characterization, it is difficult to precisely locate the centre of the fiber cross-section. Therefore the origins of the X and Z axes are somehow arbitrary and are offset from the centre of the fiber cross section by a certain amount. The extinction ratio is defined in the calculations as the ratio of the coupling efficiencies between the LP_{11a} and LP_{11b} modes. The experimental values of the extinction ratio are obtained by exciting one specific mode (either LP_{11a} or LP_{11b}) as described above and measuring the power collected by the SSMF placed at the focal point of the 10 × microscope objective as a function of the spatial coordinates X and Z. The ratio of the powers collected when LP_{11a} and LP_{11b} are excited is then calculated. Although the simulation results show that an extinction ratio larger than 20 dB can be obtained when the two modes are excited precisely, the best results obtained in the experiment for exciting the LP_{11a} and LP_{11b} modes are only 11.2 dB and 9.2 dB, respectively, due to the coarse mode launching technique and possible mode coupling, which is not considered in the calculations.

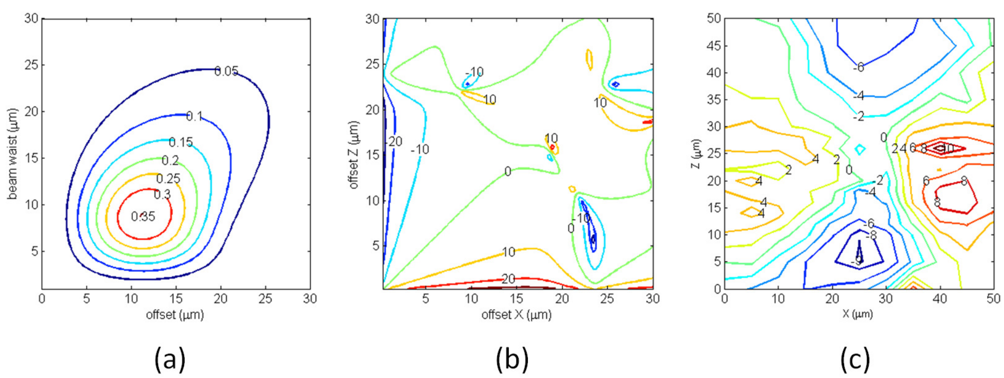

Fig. 5. (a) Simulated out-coupling efficiency as a function of radial offset and Gaussian beam waist. (b) and (c) Simulated and experimental contour plots of extinction ratio for detecting the LP_{11a} mode, respectively. The X and Z directions are shown in Fig. 3(a).

4. System performance evaluation

The experimental setup for system performance evaluation is shown in Fig. 6. A 10.7 Gbps non-return to zero (NRZ) signal is generated by modulating a continuous-wave (CW) light at 1550 nm in a Mach-Zehnder modulator (MZM). A 2^7-1 pseudo-random binary sequence length is used. Two data channels are formed by splitting the signal at the output of the MZM into two branches. Each path is controlled by a polarization controller (PC). A 500 m standard SMF is added into one of the light paths to de-correlate the two data channels. The length of the used HC-PBGF is 30 m. After transmission through the HC-PBGF link, the received signal is sent into a pre-amplified receiver for BER measurements. Figures 7(a) and 7(b) show the eye diagrams of the received LP_{11} modes without and with the other LP_{11} channel

#166096 - $15.00 USD Received 5 Apr 2012; revised 12 May 2012; accepted 12 May 2012; published 16 May 2012

switched on, resulting in BER of 10^{-9} and 3.3×10^{-3}, respectively. For comparison, the eye diagram of the received LP_{01} mode is shown in Fig. 7(c) at a BER of 10^{-9}.

Figure 7(d) shows the BER performances of the two-mode multiplexing system. The back to back case is obtained by directly connecting the output of the MZM to the pre-amplified receiver. When a single LP_{11} mode is transmitted over the HC-PBGF, power penalties of 1 and 3 dB are measured for the LP_{11a} and LP_{11b} modes, respectively. However, the BER performance degrades significantly when the other LP_{11} mode is switched on and mode multiplexing is implemented. Nevertheless, a BER below the FEC threshold (3.3×10^{-3}) assuming 7% overhead has been achieved for both simultaneously transmitted LP_{11} channels. Worse performance is obtained for the LP_{11b} mode due to its poorer extinction ratio. Such BER degradation, as well as the different performance observed between the two channels, are believed to be largely due to the non-optimized detection position in the de-multiplexing stage, as discussed in Section 3. The performance of the fundamental LP_{01} mode has also been measured. Almost no power penalty has been achieved in this case at a BER of 10^{-9}, indicating the excellent performance of the transmission using the fundamental mode at 10.7 Gbps. As can be expected from the discussion in section 2, no strong impact from dispersion is observed for both LP_{01} and LP_{11} channels in the BER measurements.

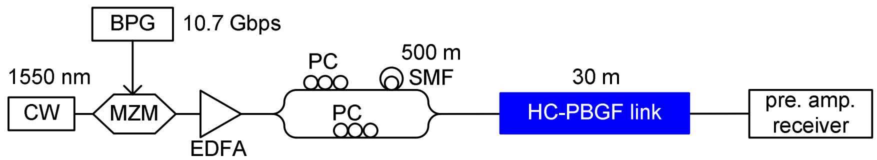

Fig. 6. Experimental setup for system evaluation.

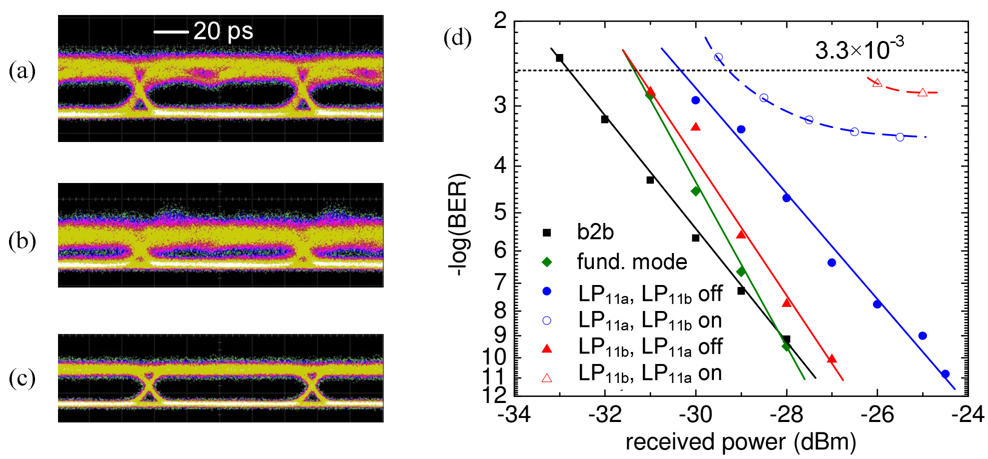

Fig. 7. Eye diagrams at the HC-PBGF output for (a) the LP_{11a} mode when the LP_{11b} mode is off, (b) the LP_{11a} mode when the LP_{11b} mode is on, (c) the fundamental mode. (d) BER performance for single mode (LP_{01}, LP_{11a} or LP_{11b}, solid symbols) as well as multimode (LP_{11a} and LP_{11b}, open symbols) transmission.

5. Conclusion

We have demonstrated for the first time a two-mode multiplexing system in a section of hollow-core photonic bandgap fiber. The optimum free space coupling implementations are validated through theoretical calculations. BER performances below the FEC threshold limit (3.3×10^{-3}) are obtained for both LP_{11} channels. Error free performance (at a BER of 10^{-9}) with a power penalty of up to 3 dB is achieved when transmitting only one single LP_{11} mode. Transmission of the fundamental mode is also characterized for comparison and results in

#166096 - $15.00 USD Received 5 Apr 2012; revised 12 May 2012; accepted 12 May 2012; published 16 May 2012

almost no power penalty at a BER of 10^{-9}. These exploratory experimental results agrees well with estimated fiber characteristics and crosstalk expectations and are believed to be improved greatly by upgrading the mode multiplexing and demultiplexing methods. Better performance is expected if more sophisticated mode matching techniques are used [3–7,21], as well as by employing specifically designed HC-PBGFs [22].

Acknowledgments

The authors would like to thank Radu Malureanu for providing the infrared camera. This work is supported by the Danish Council for Technology and Productions Sciences (project 10-093299).